
Intra-Procedural Coronary Intervention Planning Using Hybrid 3-Dimensional Reconstruction Techniques¹

Onno Wink, MS, Richard Kemkers, MS, Shih-Yung J. Chen, PhD, John D. Carroll, MD

Rationale and Objectives. The purpose of this study was to develop a method to assist the cardiologist in planning an interventional procedure while the patient is on the catheterization table.

Materials and Methods. A rotational single plane x-ray system is used to acquire images while rapidly rotating the C-arm around the patient. Based on electrocardiogram-selected projections, both a volumetric cone-beam reconstruction of the coronary tree as well as a three-dimensional model of the vessel segment of interest is generated. This information is used to compute the appropriateness of a range of different viewing angles with respect to the overlap and foreshortening of the vessel segment of interest during the cardiac cycle which results in an interactive optimal view map.

Results. The proposed method has been tested on patient data and several phantom objects. The results show that both an accurate 3D model of a vessel segment of interest and its associated optimal view map can be generated to predict an appropriate gantry angle for subsequent image acquisition.

Conclusion. The method provides an appropriate and feasible tool to assist interventional cardiologists in planning a coronary intervention while the patient is still on the catheterization table following diagnostic coronary angiography.

Key Words. Rotational coronary angiography; coronary modeling; cone-beam back-projection; intervention planning.

© AUR, 2003

Coronary artery disease remains the major cause of morbidity and mortality in the United States. Over the past years, there has been a marked increase in the number of catheterization procedures performed. This number is expected to further increase because of recent advances in stent technology (eg, drug-eluting stents, imaging capabilities, and an aging of the population). Coronary catheter-

izations are currently performed using x-ray angiography. Choosing the correct stent dimensions is often difficult using the traditional two-dimensional projection images because of vessel foreshortening and overlap. Based on the specific anatomy of the coronary branch and skill of the clinician, several angiographic images from different viewing angles are acquired to derive the length and diameter of the stent to be used for subsequent intervention. Once the clinician decides on the stent dimensions, a "working view" is chosen for the actual interventional procedure. In this view, it is expected that the vessel segment of interest is the least foreshortened and not blocked from sight. This trial-and-error method of selection of appropriate viewing angles potentially exposes the patient to large amounts of contrast medium (dye) and radiation, even before the actual treatment of the patient begins.

Acad Radiol 2003; 10:1433-1441

¹ From Philips Medical Systems North America, Cardiovascular X-ray, Bothell, WA, 98021 (O.W., R.K.); and the Department of Medicine, Division of Cardiology, University of Colorado Health Sciences Center, Denver, CO (S.-Y.J.C., J.D.C.). Received May 20, 2003; revision requested August 28; received in revised form September 8, 2003; accepted September 9, 2003.

Address correspondence to O.W.

© AUR, 2003

doi:10.1016/S1076-6332(03)00540-3

To avoid the trial-and-error approach, several researchers have proposed various methods to construct a three-dimensional (3D) representation of the coronaries using two or three acquisitions from different viewing angles (1–11). It is the general consensus that considerable user interaction is required to construct a representation (model) of the entire coronary tree if at all possible. However, once this is accomplished, the clinician has the ability to view the entire 3D coronary tree from any angle and to choose the optimal working view without the use of extra radiation or dye. In the majority of these methods, however, the focus lies on constructing an accurate 3D model that is considered to be more accurate than the standard two-dimensional quantitative coronary analysis. A number of groups have proposed different methods to facilitate the process to determine a viewing angle that provides the least foreshortened orientation of the vessel segment of interest. Only a few groups have addressed the possibility to automatically determine a viewing angle that provides a clear (non-overlapping) view of the vessel segment of interest.

Recently, rotational angiography (RA) has proven to be a very accurate and effective diagnostic tool in the treatment of cerebral vessel malformations. In this approach, the C-arm rotates rapidly around the patient while several x-ray projections are acquired. The reconstructed vessels can be viewed from different viewing angles, while only one contrast injection is given. Because of the high reproducibility of the rotational acquisitions, the fast rotation speed, and static nature of the cerebral vessels, all the projections can be used for volumetric reconstruction providing very high detail and accurate anatomic information (12). In addition, the computation is completely automated. It has been shown that the use of RA for coronary vessel acquisitions yields better stenosis severity estimations and reveals lesions that were missed by only applying the traditional acquisitions (13) and significantly reduces the amount of contrast and radiation administered to the patient (14). However, straightforward volumetric reconstruction of coronary arteries suffers from the beating of the heart and respiratory motion (15) yielding only a rough representation of the coronaries (see also Fig 3). Although recent developments with alternative reconstruction schemes (16) or based on an automated approximation of the 3D central axis (17) are very promising, an accurate reconstruction for quantifying the true dimensions of a lesion in human coronary subjects is not yet available.

Exciting new advances in other imaging modalities such as cardiac magnetic resonance and multi-detector cardiac computed tomography are arising. Currently, however, only the major coronary arteries can be visualized using these new modalities. In addition, the use of this type of modalities is usually hampered by the need for an additional alignment or registration process if it is used for an intervention in the cardiac catheterization laboratory.

In this article, a method is proposed that combines the complementary features of volume- and surface-based reconstruction techniques (see also Wink et al (18)). The rotational acquisition is used to minimize contrast medium and x-ray exposure. The projections corresponding to the same phase of the cardiac cycle are used to create an accurate surface-based model of the coronary segment of interest and to create a volumetric representation of the main coronary vessels. Through the use of an optimal view map based on the hybrid reconstruction, a viewing angle can be derived that minimizes the overlap and foreshortening and which can be used for subsequent interventions.

The proposed method is unique in several ways. The manual creation of a surface model of human coronary arteries based on projections from a rotational acquisition has not been demonstrated before. Consequently, the method is unique in the fact that it allows a model to be built based on every projection that is acquired at the same time point in the cardiac cycle. Furthermore, to the best of our knowledge, volumetric reconstructions of the main coronary arteries of actual patients with the use of a single C-arm system have not been shown before. In addition, the automated volumetric reconstructions provides a 3D visualization of the main vessels in the coronary tree and facilitates the assessment of overlap throughout the cardiac cycle without the need to manually create a surface model of the entire coronary tree.

MATERIALS AND METHODS

After the x-ray projections are acquired using a rotational C-arm system (Integris Allura 12 inch monoplane; Philips Medical Systems, Best, The Netherlands), the images are sent to a workstation (Octane; Silicon Graphics Inc, Mountain View, CA). Based on the electrocardiographic signal, two projections are chosen that correspond to the same phase of the cardiac cycle to create the central vessel axis followed by the instantaneous computation

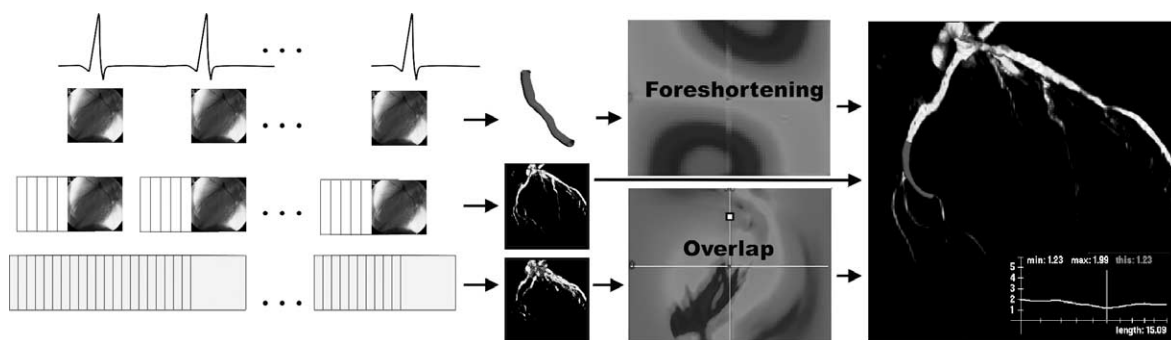


Figure 1. Flow of the method resulting in the dimensions of a coronary segment, a visualization of the coronary tree, and an optimal viewing angle to perform the actual intervention.

of the foreshortening map. The other projections captured at the same phase can be used to refine the surface model of the segment of interest. The projections that are acquired approximately at the same phase are used to visualize the coronary tree, while all the acquired projections are used to compute the overlap map. In Figure 1, a schematic description of the flow is given.

Acquisition

The C-arm is placed at the head-position of the table to perform a rotational (propeller) run from 120 RAO (right side of patient) to 120 LAO (left side of patient). The C-arm rotates at 55°/second and acquires images at 30 frames per second during 4 seconds while the patient is asked to hold his/her breath. A total of 8 to 12 cc's of contrast medium (Omnipaque 350; Novation, LLC, Omnipaque 30, Amersham plc, Buckinghamshire, UK) is used during the acquisition, while the injection is started at the moment the gantry begins to rotate. Because the rotational acquisition has been calibrated at an earlier stage (12), the individual projections are corrected for the influence of the earth magnetic field and the pincushion distortion followed by an automatic transformation to a common world coordinate system.

Coronary Modeling

Based on the electrocardiographic signal, the projections that correspond with the same phase of the cardiac cycle are chosen to model the segment of the artery of interest. Generally the end-diastolic phase of the heart is used because of the relatively steady location of the coronaries in that phase.

To construct the central axis, two projections are chosen where the segment of interest is clearly visible and the angle between the two projections is around 90°. Be-

cause, on average, five to six heartbeats are captured during the run, two projections with a relatively clear view of the lesion (although probably foreshortened) can generally be chosen. The central axis of the arterial segment is manually identified by adding point pairs in the 2-dimensional projections. For example, a point in projection A yields an epipolar line in projection B, which is the imaginary ray coming from the x-ray source towards the point in projection A. Once a point is defined in one projection, the user has to select the corresponding point along the epipolar line in the other projection. By using this "epipolar constraint," it is guaranteed that the corresponding epipolar lines do intersect and define a point on the 3D central axis. Once the axis of the lesion is created, the user has the opportunity to delineate the borders of the lumen in every projection that corresponds to the same phase of the heart to create and refine the surface model of the lumen. The average time to create a model for a segment of interest once the pair of projections is determined is less than 15 seconds on the workstation. In Figure 2, a snapshot of the user-interface is shown.

In the snapshot, we employed two projections as displayed at the lower right panel in Figure 2, chosen by the user based on the electrocardiographic signal and their relative angles. Two epipolar lines that correspond to the beginning of the segment of interest are shown. In the upper left image, the model is shown together with a volumetric representation of the coronary tree. In the upper right image, the 3D central axis is projected back to another projection out of the same rotational run that corresponds to the same phase of the heart. The dimensions of the 3D model are displayed in a graph. For a detailed discussion regarding the two views based coronary modeling, please refer to Chen and Carroll (6).

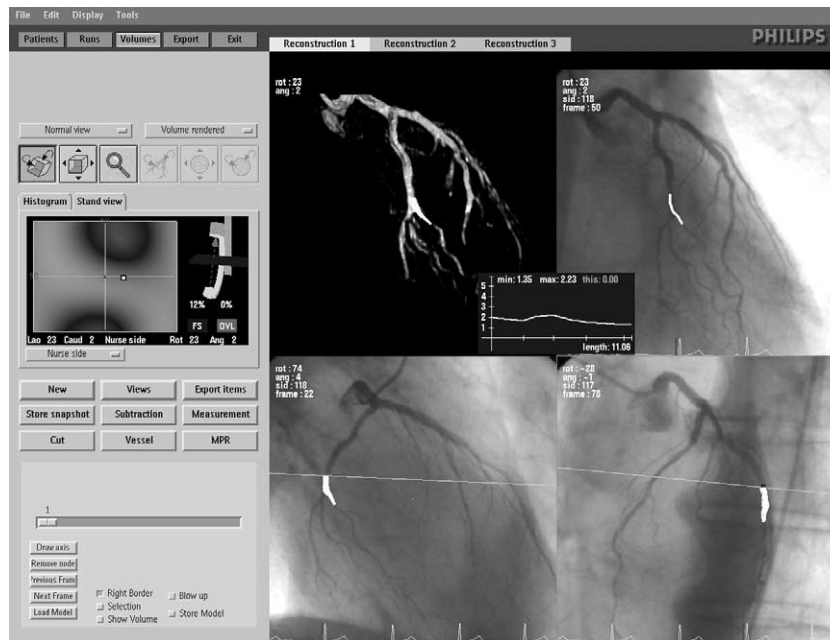


Figure 2. Snapshot of the user-interface (enhanced for gray-scale display), showing different projections that correspond to the same phase of the heart as well as a hybrid visualization of the modeled segment and a volumetric reconstruction of the coronary tree. The graph depicting the length and the average diameter of the segment of interest is displayed in the middle of the screen, while the view map and a chosen gantry position are shown in the left column.

Volumetric Reconstruction

An adapted version of the Feldkamp back-projection (19) algorithm is applied for the volumetric reconstruction. The projections are weighted according to the speed of the C-arm, where the projections acquired at a constant rotation speed have a higher weight than those acquired during startup and slowing down of the C-arm. If all of the 120 available projections are used, the resultant reconstruction contains information about the location of the coronary arterial tree throughout the cardiac cycle, and is often difficult to interpret, as can be appreciated in Figure 3.

To facilitate visualization and inspection of the coronary arteries, only those projections are used in the reconstruction process that correspond to the same cardiac cycle used to build the surface model of the vessel segment of interest. In the rightmost frame in Figure 1 and upper left frame of Figure 2, the partial reconstructions of the same coronary tree are shown.

Optimal Viewing Angle Determination

The view that is chosen to be used during the intervention (working view) is based on a combination of the amount of foreshortening of the segment of interest and

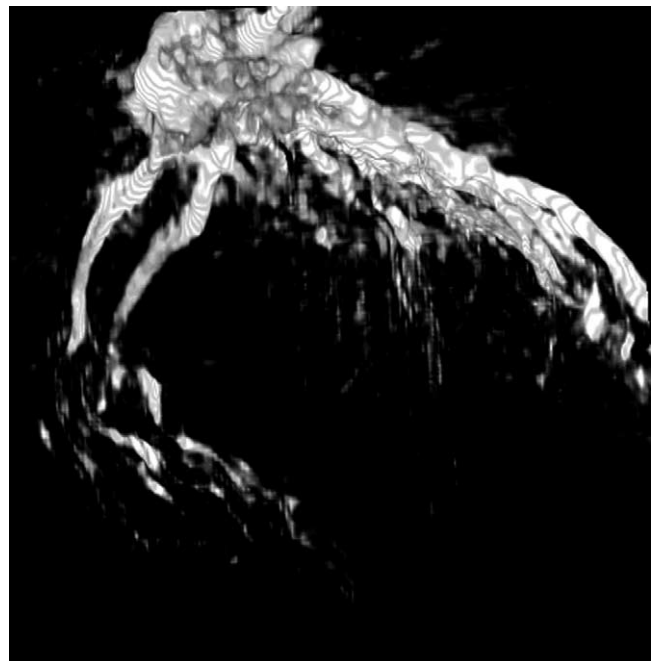


Figure 3. Straightforward volumetric reconstruction using all 120 projections from the rotational acquisition.

the overlap of other structures (5,6). Instead of computing only a single viewing angle or a limited selection of viewing angles through a plane orthogonal to the lesion of interest, the appropriateness of a large range of different viewing angles is displayed in an interactive color coded map (6). In the examples used in this article, a green color (light grey) in the map corresponds to the best viewing angle while the red color (dark grey) corresponds to the worst viewing angle. The left of the map corresponds to a RAO position, while the top of the map corresponds to a cranial position (toward the head of the patient). The user can inspect the different viewing angles in the map by clicking at a position in the map and to toggle between the different types of maps. The amount of foreshortening and overlap that correspond to the user selected viewing angle are shown in the user interface, in addition to a model of the corresponding configuration of the C-arm gantry.

For a practical application of the optimal view map, only the mechanically achievable gantry angles are computed. In general, the cranial and caudal angulation should not exceed 45° from the anterior-posterior plane while the RAO and LAO rotation is limited to 60° to reduce the possibility of contact between the image intensifier and the patient. For a detailed description of the different maps please refer to Chen and Carroll (6).

Foreshortening map.—The foreshortening map is computed by comparing the length of the modeled segment to its projected length as if it were viewed from a typical viewpoint as defined by the range of angles in the map.

Overlap map.—Although the volumetric reconstruction of all the acquired projections yields only a rough representation of the coronaries, it does provide information where the vessels and other objects (eg, the spine, ribs, sternum wires, and pacemaker or electrocardiogram-leads) are located during all the phases of the heart. The overlap map is computed by taking the integral of all the grey values from the reconstructed volume along the rays that intersect the modeled segment. This is very efficiently implemented in OpenGL using space-leaping techniques and the Stencil Buffer (20) in combination with the special purpose graphics hardware of the SGI Octane.

Optimal view map.—The optimal view map can be constructed by taking a weighted sum of normalized values of the foreshortening map and overlap map (see Fig 4).

One of the strengths of the optimal view map is that the clinician has the flexibility to interactively explore

multiple potential working views for subsequent diagnostic or therapeutic treatment. For a practical implementation and efficient computation, the vessel overlap is generally calculated for those gantry angles where the vessel foreshortening has been minimized or is less than 15% to obtain the optimal working view.

RESULTS

In this section, two phantoms and a marked catheter with known dimensions are used to assess the accuracy of both length and diameter as well as the correctness of the overlap map. Also, some results of the method when applied to patient data are given to show the clinical benefit of the proposed approach. In all studies, the contents of the maps are computed between 90 RAO and 90 LAO and 90 Cranial and 90 Caudal. The optimal view map is computed using an equally weighted sum of the foreshortening and overlap map.

Perspex Phantom

The phantom used is a perspex cube of $3 \times 3 \times 3$ cm containing three aluminum rods with a diameter of 2 mm, oriented in the three main directions and three spheres with a diameter of 3 mm as shown in the leftmost frame of Figure 5. The 13th and 63rd projection are chosen from the rotational acquisition to model the rod that is vertically positioned. To quantify the accuracy, four borders are carefully drawn to define the associated diameter of the rods. All the projections are used to reconstruct the volume for both visualization and computation of the overlap map. The projection corresponding to the worst viewing angle is shown in the right frame of Figure 5.

From the hybrid visualization in the rightmost frame of Figure 5, it can be derived that the generated model is very similar to the results of the volumetric reconstruction. Four different propeller acquisitions are performed with the image-intensifier set to 12, 9, 7, and 5 inches, respectively. The average diameter of the modeled rod is 1.84 mm, while the average length of the rod is 30.02 mm. The underestimation of the diameter of the rod can be explained by the reduced contrast between the material of the rod and its surrounding material.

Coronary Phantom

The coronary phantom is a copy of the so called "toiletball" phantom used in earlier studies to determine the accuracy of the length and diameter estimation using a similar version of the coronary modeling algorithm (21).

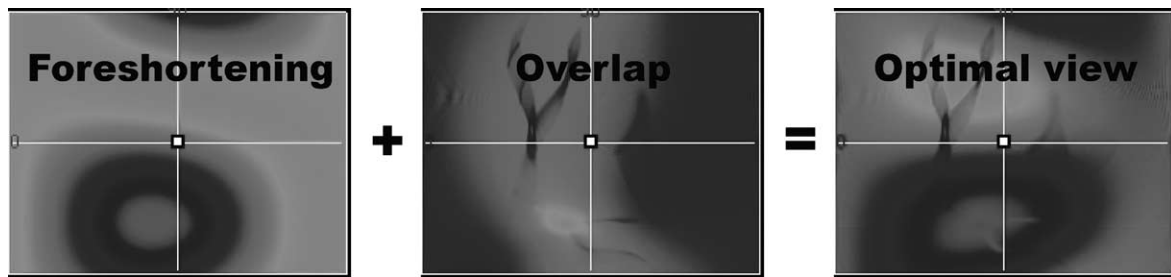


Figure 4. Example of the construction of an optimal view map based on a foreshortening and overlap map.

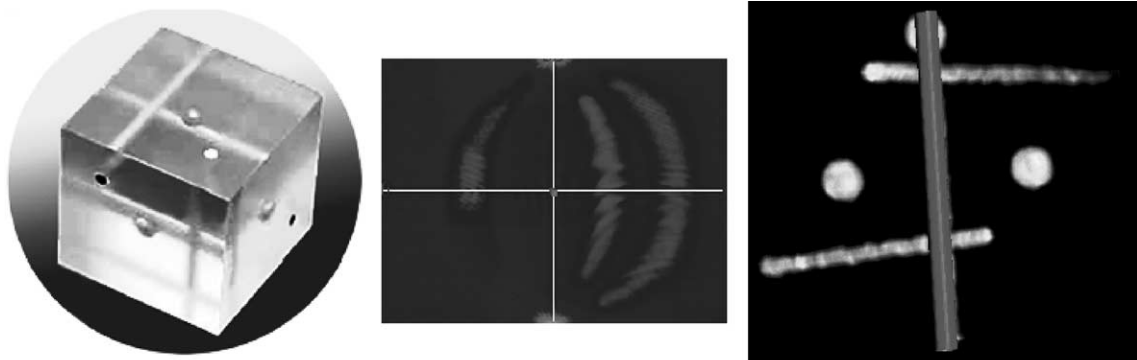


Figure 5. The perspex phantom (left frame). The overlap map (middle frame), clearly displaying the “orbits” of the spheres where they are overlapping with the rod of interest. Hybrid visualization of the modeled (vertical) rod and re-constructed phantom having the most overlap (right frame).

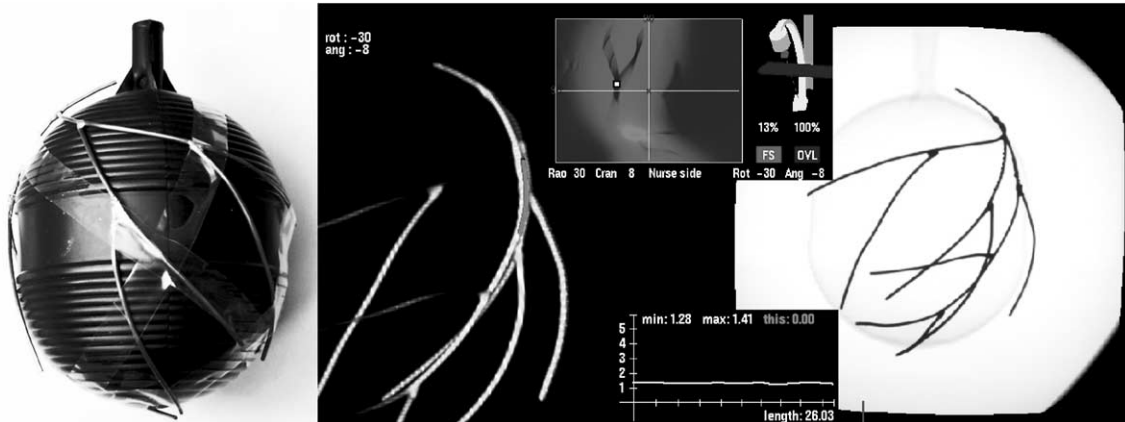


Figure 6. The “toiletball” phantom (left frame). In the right composite figure, the hybrid visualization of the worst overlapping position is shown.

The plastic floater is used as a base for the copper wires with a diameter of 1.5 mm, which represent a simple coronary tree (see left frame of Fig 6).

In Figure 6, the graph shows that the diameter of the copper wire is estimated to be around 1.5 mm. The central axis of the computed model is displayed in the x-ray projection to show that good correspondence is achieved. The optimal view map shows that there are only very

small regions where ‘vessels’ are overlapping. The maps in Figure 4 correspond to the same segment of this phantom.

Marked Catheter

A marked catheter (Cook Royal Flush II pigtail) is placed in the left ventricle of the heart of two patients. The catheter has two radio-opaque markers at the tip that

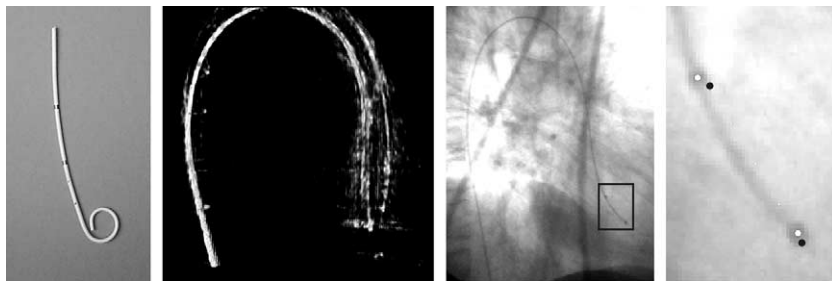


Figure 7. The catheter with the radio-opaque markers (leftmost frame); the volumetric reconstruction displaying the movement of the catheter tip (middle left frame); and a projection displaying the markers while positioned in the left ventricle of a patient (middle right frame). The determination of the accuracy of the projected 3D position of the markers (black dots) compared with the manually determined position of the markers (white dots in rightmost frame).

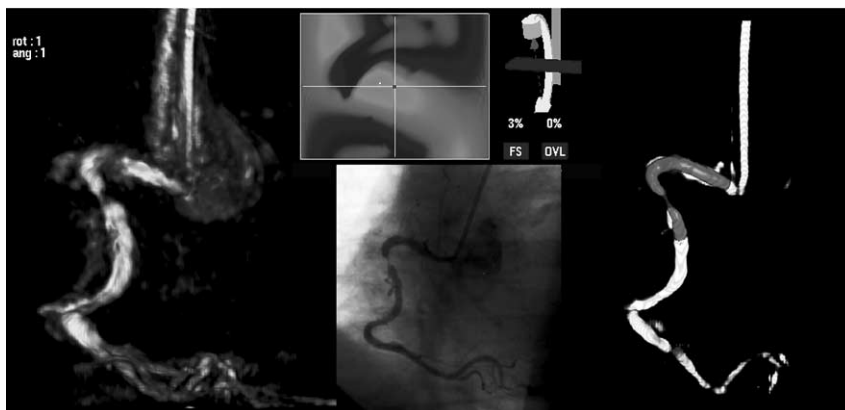


Figure 8. Example of a patient with a very severe stenosis in the right coronary artery.

are 22 mm apart (see left frame of Fig 7). Based on two projections, A and B, from the rotational acquisitions using an II-size of 12 in, the 3D location of the markers is determined. The resultant 3D position is projected on the third projection (C) that corresponds to the same phase of the heart as projections A and B. The average difference between the projected 3D points and the position of the corresponding markers in projection C for both patients is 3.52 pixels.

Examples on Real Patients

In Figure 8, the results are shown for a patient with a very severe stenosis at the proximal right coronary artery. The acquisition was performed with an image intensifier (II) size of 9 in. In the left frame, all 120 projections are used for the volumetric reconstruction. In the rightmost frame, a hybrid representation is shown based on the optimal viewing angle. The optimal view map and one of the

x-ray projections of the rotational run are shown in the middle as a reference.

In Figure 9, the volumetric reconstruction of the patients left coronary arterial tree and an artificial heart valve is shown. The acquisition was performed with an II size of 12 in. In the left frame, all of the 120 projections are used for the volumetric reconstruction. Some streaking artifacts occur because the opacity of the sternum wires and the heart valve. In the rightmost frame, a hybrid representation is shown from the optimal viewing angle. The optimal view map and one of the x-ray projections of the rotational run are shown as a reference. In the hybrid representation, both the heart valve and parts of the sternum wires are reconstructed. The optimal view map yields a viewing angle that gives a clear view on the lesion of interest. In this example, the result show that the volumetric reconstruction of non-vessel objects is well suited to derive the optimal working view.

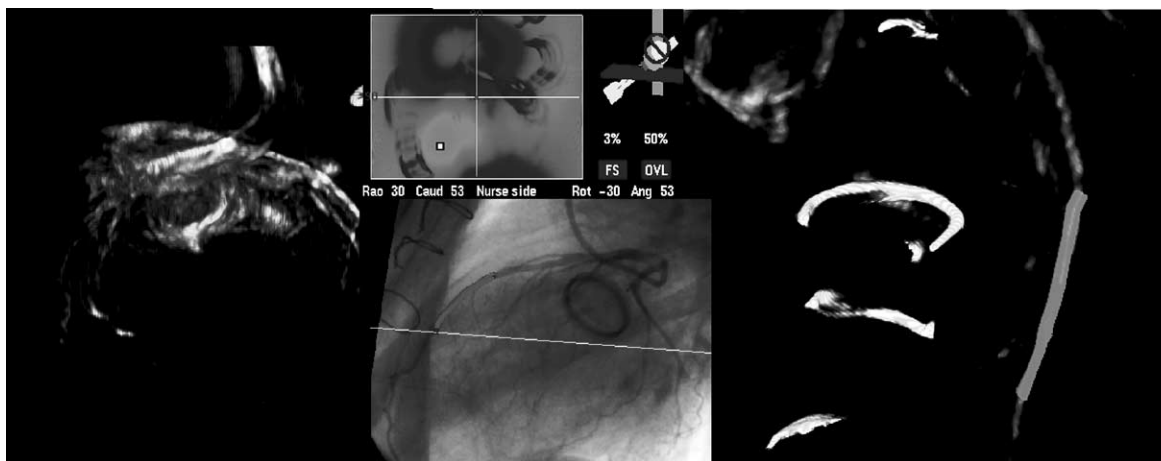


Figure 9. The exemplar image of a patient's left coronary system and an artificial heart valve. The optimal view map clearly shows the regions where the heart valve would block a user defined vessel segment of interest. In the optimal view, the reconstructed heart valve is shown in the top left corner of the right image. Some partially reconstructed sternum wires are also clearly visible.

DISCUSSION

A hybrid reconstruction scheme is proposed that provides the clinician with the 3D quantitative measurement of an arterial segment and an optimal working view throughout the cardiac cycle. After the transfer of the projection images to a digital workstation, this information can be provided in less than a minute. As a result, the method can be used to plan the coronary intervention while the patient is still on the catheterization table.

The accuracy of the method is validated using two static phantoms and a marked catheter placed in-vivo. The study found the modeling approach to be accurate if the segment of interest is clearly visible in the different projections that correspond to the same time point in the heart cycle.

Although the method has been tested on more than 40 patients, the presumed added value has not yet been proven in a randomized on-line study. Therefore, we can only assume that it will positively affect the clinician decision-making process.

We believe that the representation of the value of the different viewing angles using the interactive map provides an intuitive tool that could be applied to virtually any vessel in the human body. Furthermore, we are convinced that there is a lot of potential in the combination of the two types of reconstructions that will be worth investigating, especially in the analysis of coronary arteries.

ACKNOWLEDGMENTS

The authors thank Rolf Suurmond, Paul Desmedt, and Wiet Lie from Philips x-ray pre-development in Best, The Netherlands, for their active support in creating the prototype environment. The authors also thank Babak Movasaghi and Reiner Koppe from Philips Research Laboratories in Hamburg for their help on calibration issues. The authors also thank the many anonymous patients who consented to the use of their image data.

REFERENCES

1. Dumay ACM, Reiber JHC, Gerbrands JJ. Determination of optimal angiographic viewing angles: basic principles and evaluation study. *IEEE Trans Med Imaging* 1994; 12:13-24.
2. Solzbach U, Oser U, Romback M, Wollschläger H, Just H. Optimum angiographic visualization of coronary segments using computer-aided 3D reconstruction from biplane views. *Comput Biomed Res* 1994; 27: 178-198.
3. Wahle A, Wellnhofer E, Mugaragu I, Sauer HU, Oswald H, Fleck E. Assessment of diffuse coronary artery disease by quantitative analysis of coronary morphology based upon 3D reconstruction from biplane angiograms. *IEEE Trans Med Imaging* 1995; 14:230-241.
4. Klein JL, Hoff JG, Peifer JW, Folks R, Cooke CD, King SB III, Garcia EV. A quantitative evaluation of the three dimensional reconstruction of patient's coronary arteries. *Int J Cardiac Imaging* 1998; 14:75-87.
5. Sato Y, Araki T, Hanayama M, Naito H, Tamura S. A viewpoint determination system for stenosis diagnosis and quantification of coronary angiographic image acquisition. *IEEE Trans Med Imaging* 1998; 17: 121-137.
6. Chen YJ, Carroll JD. Computer assisted coronary intervention by use of on-line 3D reconstruction and optimal view strategy. *Proc Med Image. Comput Computer Assisted Intervention*, Cambridge, MA. October 1998. Berlin: Springer; 377-385.
7. Rivas R, Ibáñez MB, Cardinale Y, Windyga P. A parallel algorithm for

- 3D reconstruction of angiographic images. *Future Gene Comput Syst* 2000; 16:533–539.
8. Chen J, Carroll JD. 3D reconstruction of coronary arterial tree to optimize angiographic visualization. *IEEE Trans Med Imaging* 2000; 9:318–336.
 9. Sarry L, Boire J-Y. Three-dimensional tracking of coronary arteries from biplane angiography sequences using parametrically deformable models. *IEEE Trans Med Imaging* 2001; 20:1341–1351.
 10. Christiaens J, Van de Walle R, Gheeraert P, Taeymans Y, Lemahieu I. Determination of optimal viewing angles for QCA. *Computer Assisted Radiology and Surgery*, Berlin, Germany. June 2001. *Comput Assist Radiol* 2001; 31:865–870.
 11. Kayikcioglu T, Gangal A, Turhal M. Reconstructing coronary arterial segments from three projection boundaries. *Pattern Recogn Lett* 2001; 22:611–624.
 12. Koppe R, Klotz E, op de Beek J, Aerts H. Digital stereotaxy/stereotactic procedures with C-arm based rotational-angiography (RA). *Comput Assist Radiol* 1996; 31:17–22.
 13. Tommasini G, Camerini A, Gatti A, Derchi G, Bruzzzone A, Vecchio C. Panoramic coronary angiography. *JACC* 1998; 31:871–877.
 14. Kuon E, Niederst PN, Dahm JB. Usefulness of rotational sping for coronary angiography in patients with advanced renal insufficiency. *Am J Cardiol* 2002; 90:369–373.
 15. Rougée A, Picard C, Saint-Félix D, Troussset Y, Moll T, Amiel M. Three-dimensional coronary arteriography. *Int J Cardiac Imaging* 1994; 10:67–70.
 16. Rasche V, Buecker A, Grass M, et al. ECG-gated 3D-rotational coronary angiography. *Computer Assisted Radiology and Surgery*, Paris, France. June 2002.
 17. Blondel C, Vaillant R, Devernay F, Malandain G, Ayache N. Automatic trinocular 3D reconstruction of coronary artery centerlines from rotational X-ray angiography. *Computer Assisted Radiology and Surgery*, Paris, France. June 2002.
 18. Wink O, Kemkers R, Chen SJ, Carroll JD. Coronary intervention planning using hybrid 3D reconstruction. *Proc Medical Image Computing and Computer-Assisted Intervention*, Tokyo, Japan. September 2002. Berlin: Springer; 2002.
 19. Feldkamp LA, Davis LC, Kress JW. Practical cone-beam algorithms. *J Opt Soc Am* 1984; 6:612–619.
 20. Woo M, Neider J, David T, Shreiner D. *OpenGL Programming Guide*, Version 1.2. Reading, MA, Addison Wesley, 1999.
 21. Messenger JC, Chen SYJ, Carroll JD, Burchenal JEB, Kioussopoulos K, Groves BM. 3D coronary reconstruction from routine single-plane coronary angiograms: clinical validation and quantitative analysis of the right coronary artery in 100 patients. *Int J Cardiac Imaging* 2000; 16:413–427.